Neutron study of magnetic excitations in 8-nm -Fe2O3 nanoparticles

Kuhn, Luise Theil; Lefmann, Kim; Bahl, Christian Robert Haffenden; Nyborg Ancona, S.; Lindgård, Per-Anker; Frandsen, Cathrine; Madsen, Daniel Esmarch; Mørup, Steen

Published in:
Physical Review B Condensed Matter

Link to article, DOI:
10.1103/PhysRevB.74.184406

Publication date:
2006

Document Version
Publisher's PDF, also known as Version of record

Neutron study of magnetic excitations in 8-nm α-Fe_2O_3 nanoparticles

L. Theil Kuhn,* K. Lefmann, C. R. H. Bahl,[†,‡] S. Nyborg Ancona,[§] and P.-A. Lindgård
Materials Research Department, AFM-228, Risø National Laboratory, DK-4000 Roskilde, Denmark

C. Frandsen, D. E. Madsen, and S. Mørup
Department of Physics, Building 307, Technical University of Denmark, DK-2800 Kongens Lyngby, Denmark
(Received 9 June 2006; revised manuscript received 11 September 2006; published 3 November 2006)

By use of inelastic neutron scattering we have studied magnetic fluctuations in 8-nm particles of antiferromagnetic α-Fe_2O_3 (hematite) as a function of temperature and applied magnetic fields. The fluctuations are dominated by uniform excitations. Studies have been performed on both coated (noninteracting) and uncoated (interacting) particles. We have estimated the magnetic anisotropy energy and found that the data are in good agreement with the value obtained from Mössbauer spectroscopy. The energy ε_0 of the uniform excitations depends strongly on the uncompensated moment, which is caused by finite-size effects, and we have estimated the size of this moment from the experimental neutron data. The field dependence of ε_0 for the interacting nanoparticles differs strongly from that of the noninteracting nanoparticles, and this is a result of the influence of exchange interaction between the particles.

DOI: 10.1103/PhysRevB.74.184406 PACS number(s): 75.50.Tt, 75.30.Ds, 75.30.Gw, 25.40.Fq

I. INTRODUCTION

Materials composed of nanoscale magnetic grains are becoming important in technological applications, since they provide the possibility of designing materials with new magnetic properties. This is indeed true for magnetic nanoparticles used in, for example, ferrofluids, biomedicine, hard permanent magnets and magnetic recording media.[1,2] Understanding the fundamental properties of the grains and the influence of magnetic interactions is therefore of great importance.

The magnetic anisotropy of a single nanoparticle is in the first approximation assumed to be uniaxial with the anisotropy energy given by

$$E(\theta) = KV \sin^2 \theta, \tag{1}$$

where K is the magnetic anisotropy constant, V is the particle volume, and θ is the angle between the (sublattice) magnetization and an easy direction of magnetization. KV is the energy barrier that separates the two minima at $\theta=0$ and $\theta=\pi$. If the thermal energy is comparable to KV, superparamagnetic relaxation takes place, i.e., the magnetization vector fluctuates between the easy directions of magnetization.[3] At lower temperatures the magnetization vector fluctuates in directions close to one of the easy axes, i.e., performs collective magnetic excitations.[4,5] These magnetic fluctuations can be described as a uniform precession (a spin wave with wave vector $q=0$) of the magnetization vector around an easy direction of magnetization in combination with transitions between these precession states. Due to finite-size quantization there is a large energy gap in the spin wave spectrum to the spin waves with $q \neq 0$. The spin wave spectrum is discrete[6,7] and excitations of the uniform ($q=0$) mode are therefore predominant.[8]

Interactions between magnetic nanoparticles can have a strong influence on the magnetic properties. For ferromagnetic and ferrimagnetic nanoparticles, the interparticle dipole interaction can have a significant influence on the superparamagnetic relaxation time, see, e.g., Refs. 9–16. Nanoparticles of antiferromagnetic materials have recently attracted much attention because their properties in several ways differ from those of the bulk materials. They have a nonzero magnetic moment, which has been attributed to uncompensated spins,[17,18] but recently it was suggested that it also can have a contribution from so-called thermoinduced magnetization.[19] An anomalous temperature dependence of the magnetic moments, which has been observed in several studies[20–23] seems to support this, but may also be explained by shortcomings in the analysis of magnetization data for antiferromagnetic nanoparticles.[24] Macroscopic quantum tunneling of the magnetization, which is characterized by a temperature-independent relaxation, is expected to be more pronounced in antiferromagnetic nanoparticles than in ferromagnetic and ferrimagnetic nanoparticles.[25] Such a temperature-independent relaxation has been observed in low-temperature studies of, for example, ferritin[26,27] and α-Fe_2O_3 nanoparticles.[28] Other studies have shown that the magnetic structure of, for example NiO nanoparticles may differ from the bulk magnetic structure.[29] In α-Fe_2O_3 nanoparticles, the Morin transition is suppressed[30,31] and the spin-flop field decreases with decreasing particle size.[32] In samples of antiferromagnetic nanoparticles the interparticle dipole interactions are negligible, because the magnetic moments of the particles are small,[33] but the exchange coupling between surface atoms of nanoparticles in close contact may be a prominent source of interaction effects.[5,33–37]

In an atomic scale model for the interaction, we assume that the particles are magnetically coupled via exchange interaction between pairs of surface ions. The magnetic interaction energy of a particle p with surface spins $\mathbf{S}_i^p$ may be written

$$E_{\mathrm{ex}} = -\sum_i \mathbf{S}_i^p \cdot \sum_q \sum_j J_{ij}^q \mathbf{S}_j^q, \tag{2}$$

where $\mathbf{S}_j^q$ are the surface spins of the neighboring particles q and J_{ij}^q is the exchange coupling constant related to the inter-

action between the surface ions i of the particle p and the surface ions j of the neighboring particles q. Neglecting surface spin canting, we may write

$$\sum_j J_{ij}^q \mathbf{S}_j^q = A_q \mathbf{M}_q, \tag{3}$$

where $\mathbf{M}_q$ is the (sublattice) magnetization of the particle q and A_q is an effective interaction constant. Because $\Sigma_i \mathbf{S}_i^p$ is proportional to the (sublattice) magnetization $\mathbf{M}_p$ of the particle p, the total energy density may be written[5,33–36]

$$E_i = K_i \sin^2 \theta_i - \mathbf{M}_p \cdot \sum_q J_{pq} \mathbf{M}_q, \tag{4}$$

where J_{pq} is an effective exchange coupling constant.

If the first term in Eq. (4) is predominant, superparamagnetic relaxation of the individual nanoparticle may take place between the easy directions close to $\theta=0$ and $\theta=\pi$. However, if the interactions are significant, the energy at the two minima will differ and the populations will therefore differ. At finite temperatures, the (sublattice) magnetization may then mainly fluctuate around the direction corresponding to the lower energy minimum. The magnetic properties of interacting particles have been calculated by use of a simple mean field model in which the summation in the second term in Eq. (4) is replaced by an average value, which may be considered as an effective interaction field.[33–36]

Interaction effects in samples of magnetic nanoparticles have mainly been studied by ac and dc magnetization measurements and by Mössbauer spectroscopy, which together cover about 10 decades of relaxation times down to $\approx 10^{-10}$ s. It has been demonstrated that inelastic neutron scattering also is a very useful method for investigating spin dynamics in magnetic nanomaterials because the time scale of this technique expands the observable time range down to 10^{-14} s.[7,38–43] In the inelastic neutron scattering experiments the energy distribution of the neutrons, which are scattered at momentum transfer corresponding to an antiferromagnetic reflection, is measured. The neutrons can excite or de-excite a $q=0$ spin wave and thereby spin excitations can be probed.

In this paper we present the results of an inelastic neutron scattering study of coated and uncoated nanoparticles of α-Fe_2O_3 with a mean size of 8 nm. We assume that the coated nanoparticles can be treated as individual, noninteracting, particles, whereas the uncoated nanoparticles interact via exchange interactions within agglomerates. The study shows that interparticle exchange interactions between the α-Fe_2O_3 nanoparticles can have a strong effect on collective magnetic excitations. We compare the results with data obtained by Mössbauer spectroscopy on the same nanoparticle samples.

II. SPIN DYNAMICS IN HEMATITE NANOPARTICLES

α-Fe_2O_3 has the corundum crystal structure, and we describe the structure using the hexagonal unit cell. α-Fe_2O_3 nanoparticles smaller than about 20 nm in diameter are canted antiferromagnets with the spins in the (001) plane at least down to 5 K.[31] In bulk, the canting angle is approximately 0.07° and the out-of plane magnetocrystalline anisotropy is considerably larger than the in-plane anisotropy.[44] The Néel temperature of bulk α-Fe_2O_3 is $T_N=955$ K.[44] In nanoparticles, the in-plane anisotropy is larger than in bulk and may become comparable to the out-of-plane anisotropy.[7,31] Here, we will for simplicity assume that the magnetic anisotropy in α-Fe_2O_3 nanoparticles can be described as an effective uniaxial anisotropy [Eq. (1)] with anisotropy constant K_{eff}.

In noninteracting α-Fe_2O_3 nanoparticles, the amplitude of the uniform magnetic precession mode with lowest energy lies predominantly in the (001) plane,[39,43] while the second precession mode at higher excitation energy is predominantly perpendicular to the (001) plane.[7] Applied magnetic fields increase the excitation energy and hence suppress the amplitude of collective magnetic excitations. A quantum mechanical description of the details of the relaxation and precession modes can be found in Ref. 45.

In studies of magnetic nanoparticles using inelastic neutron scattering it has been found that superparamagnetic relaxation gives rise to an energy broadening of Lorentzian line shape of the magnetic Bragg reflections.[39,41,43] In the following, this will be termed the quasielastic signal. In inelastic scattering processes, the energy of the scattered neutrons can be changed by an amount ε_0 corresponding to the energy difference between two neighboring uniform precession states.[39–42] This gives rise to inelastic peaks at neutron energy transfers $\pm\varepsilon_0$. In 8-nm α-Fe_2O_3 nanoparticles, the lowest spin wave excitation with $q\neq 0$ has an energy larger than 10 meV and the antiphase $q=0$ excitation also has high energy.[6,7] Therefore, these transitions were not probed in the present measurements where only neutrons with energy transfer lower than 5 meV were detected.

The broadening of the quasielastic Lorentzian line shape due to superparamagnetic relaxation is given by[39]

$$I(\varepsilon) = D(\varepsilon) \frac{A_{\text{Bragg}}}{\pi} \frac{\Gamma}{\Gamma^2 + \varepsilon^2}, \tag{5}$$

where $D(\varepsilon)=\frac{\varepsilon}{k_b T}\left(\frac{1}{\exp(\varepsilon/k_B T)-1}+1\right)$ is the detailed balance factor, A_{Bragg} is the integrated intensity (area) of the quasielastic peak coming from the semistatic arrangement of spins, Γ is the half width at half maximum (HWHM) and is related to the lifetime of the superparamagnetic relaxation by $\Gamma=\hbar/\tau$.[41]

In previous inelastic neutron studies we have found that the damped harmonic oscillator model gives a good description of the collective magnetic excitations in both antiferromagnetic[7,39,40,43] and in ferrimagnetic nanoparticles.[42] Therefore, we will in this data analysis also apply the damped harmonic oscillator model given by[39,41,43]

$$I(\varepsilon) = D(\varepsilon) \frac{A_{\text{CME}}}{\pi} \frac{2\gamma\varepsilon_0^2}{(\varepsilon^2 - \varepsilon_0^2)^2 + 4\gamma^2\varepsilon^2}. \tag{6}$$

A_{CME} is the integrated intensity (area) of the peaks, γ is the width (HWHM) of the inelastic peaks and ε_0 is the energy difference between the precession modes. At low temperatures ($k_B T \ll K_{\text{eff}} V$) ε_0 can be approximated by[39]

$$\varepsilon_0 \approx g\mu_B\sqrt{2B_AB_E}. \quad (7)$$

$g=2$ is the g factor, μ_B is the Bohr-magneton, $B_E=900$ T is the exchange field, and B_A is the anisotropy field $B_A=K_{\text{eff}}/M_s$, where $M_s=9\times10^5$ A m^{-1} is the sublattice saturation magnetization of bulk α-Fe_2O_3.[44] The value of K_{eff} can be estimated from experimental neutron data.[7,39,41,43]

If the particles are exposed to a magnetic field, B_{appl}, which is large compared to the effective anisotropy field, the energy difference is given by[39]

$$\varepsilon_0 \approx g\mu_B B_{\text{appl}}. \quad (8)$$

In this work we analyze the data from interacting particles by use of the simple model outlined in Sec. I [Eq. (4)], where the influence of interactions is described by an effective interaction field.

The relative area of the inelastic peaks in neutron scattering experiments compared to the total magnetic scattering, also gives information on the magnetic fluctuations. For noninteracting particles with magnetic energy given by Eq. (1) the temperature dependence at low temperatures ($k_BT \ll K_{\text{eff}}V$) is given by[39,43]

$$\frac{A_{\text{CME}}}{A_{\text{Bragg}}+A_{\text{CME}}} = \langle \sin^2\theta\rangle \approx \frac{k_BT}{K_{\text{eff}}V}. \quad (9)$$

In Mössbauer spectroscopy, fast superparamagnetic relaxation results in a collapse of the magnetic hyperfine splitting, and at low temperatures ($k_BT \ll K_{\text{eff}}V$) collective magnetic excitations give rise to a reduction of the observed magnetic hyperfine field B_{obs} given by[4,5]

$$B_{\text{obs}} = B_0\langle\cos\theta\rangle \approx B_0\left(1-\frac{k_BT}{2K_{\text{eff}}V}\right), \quad (10)$$

where B_0 is the magnetic hyperfine field that would be measured in the absence of relaxation phenomena. For strongly interacting magnetic nanoparticles, Eq. (10) may be replaced by[5,33–35]

$$\langle B_{\text{obs}}\rangle \approx B_0\left(1-\frac{k_BT}{2K_{\text{eff}}V+E_{\text{int}}}\right), \quad (11)$$

where E_{int} is related to the strength of the interactions.

III. EXPERIMENTAL METHODS

The α-Fe_2O_3 nanoparticles were prepared by means of a gel-sol method similar to that developed by Sugimoto *et al.*[46] The particles resemble those described in Refs. 36, 37, 47, and 48. Part of the batch was treated with phosphate to produce a sample of particles coated with a layer of nonmagnetic material in order to minimize interparticle interactions.[42,50] For simplicity, the particles in this sample are in the following referred to as the noninteracting particles. Another part of the batch was uncoated and dried such that the particles in this sample were in direct contact. These are referred to as the interacting particles.

Transmission electron microscopy (TEM) images were obtained using a JEOL 3000F microscope, equipped with a Gatan MSC CCD-camera. TEM images are shown in Fig. 1. The particles of both samples are seen to be round with a good crystallinity. The phosphate coating is seen as an amorphous layer around the crystalline particles in Fig. 1(a). The average particle size is approximately 8 nm in accordance with x-ray and neutron powder diffraction data,[47] which also established that each particle consists of a single magnetic domain. In addition, neutron diffraction data confirmed the magnetic Bragg reflections at the scattering vectors $Q=1.37$ and 1.51 Å^{-1} corresponding to the purely antiferromagnetic (003) and (101) reflections, respectively. These data also showed that the nanoparticles are above the Morin transition in the entire measured temperature regime.

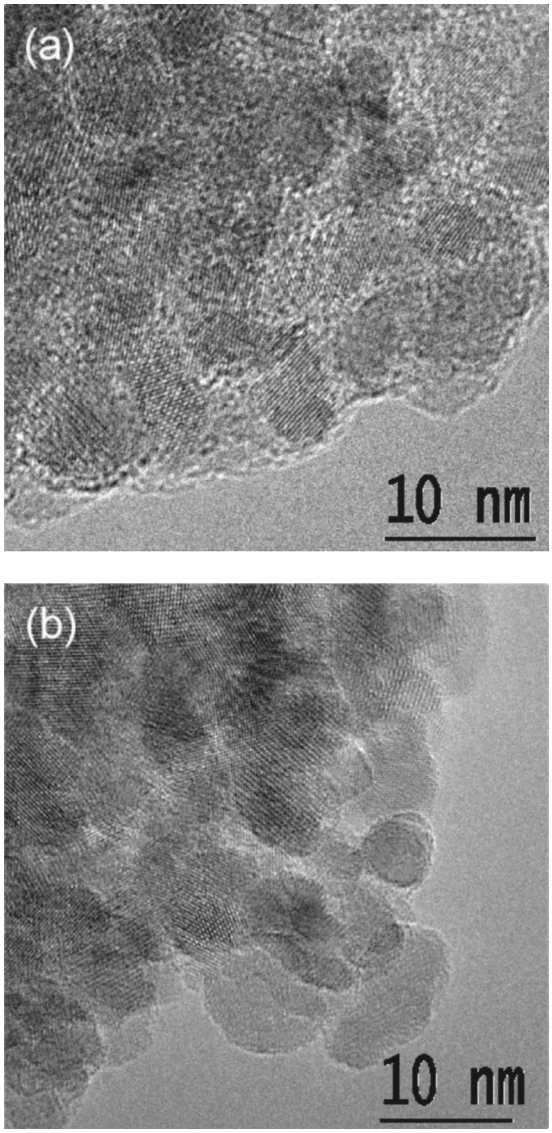

FIG. 1. TEM images of the 8-nm α-Fe_2O_3 nanoparticles. (a) The noninteracting (coated) particles and (b) the interacting (noncoated) particles. The coating is seen as an amorphous layer around the particles.

The Mössbauer spectra were obtained using constant-acceleration spectrometers with sources of ^{57}Co in rhodium. Spectra in the temperature range 18–300 K were obtained using a closed cycle helium refrigerator. Spectra at or below

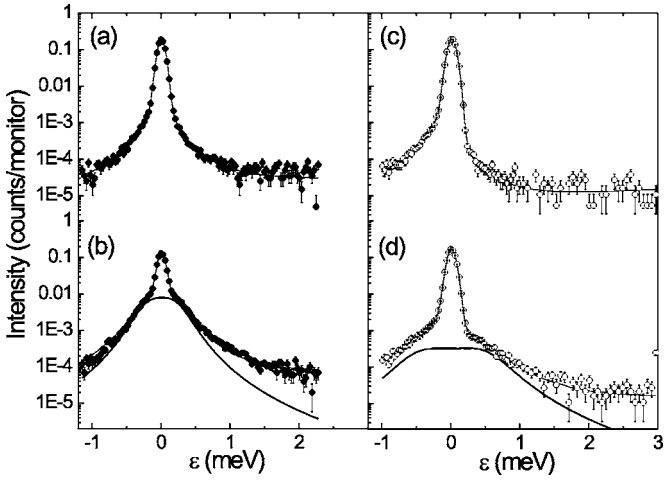

FIG. 2. Inelastic neutron data for 8-nm α-Fe_2O_3 nanoparticles. (a), (b) Energy scans with ε_f=3.7 meV at constant scattering vector τ_{003} at 10 and 150 K, respectively, for the noninteracting nanoparticles. Similar data for the interacting nanoparticles are shown in (c) and (d). The thin line represents the fit to the model as explained in the text and the bold line in (b) and (d) shows the contribution from just the collective magnetic excitations. The asymmetric tails is at $\varepsilon < 0.05$ meV are a part of the background, as explained in Sec. III. In each series of measurements, the spectra obtained at the lowest temperatures and zero applied field have been normalized to the same maximum intensity at ε_0=0 meV.

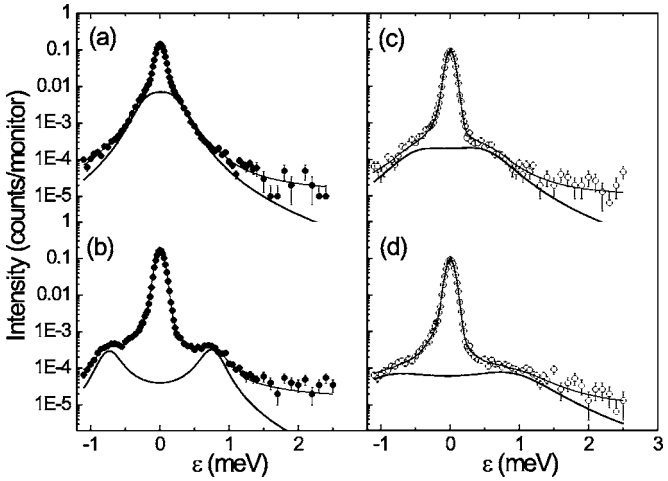

FIG. 3. Inelastic neutron data for the 8-nm α-Fe_2O_3 nanoparticles. (a), (b) Energy scans with ε_f=3.7 meV at constant scattering vector τ_{003} at 100 K at an applied magnetic field of 0 and 6 T, respectively, for the noninteracting nanoparticles. Similar data for the interacting nanoparticles are shown in (c) and (d). The thin line represents the fitted model as explained in the text, and the contribution from the just collective magnetic excitations is shown by the bold line.

18 K were obtained in a liquid helium cryostat. The spectrometers were calibrated with a 12.5-μm-thick $\alpha-$Fe foil at room temperature.

The inelastic neutron scattering experiments were performed at the cold-neutron triple-axis spectrometer RITA-2 at SINQ, Paul Scherrer Institute.[51] The experiments were performed with a 80 ′ collimator after a vertically focusing pyrolythic graphite (002) monochromator, and a radially collimating BeO filter after the sample. The final neutron energy was fixed at ε_f=3.7 meV giving an energy resolution of 80 μeV. Furthermore, spectra were also obtained for a final neutron energy of ε_f=2.9 meV. The spectrometer was run in the monochromatic point-to-point focusing analyzer mode with a position sensitive detector.[52] Following the same procedure as in Refs. 7, 39, and 43 the data were fitted using the models for superparamagnetic relaxation and collective magnetic excitations as described in Sec. II, Eqs. (5) and (6). First, the resolution function of the setup and the background function were determined from low temperature energy scans, where superparamagnetism and collective magnetic excitations are negligible, and from background energy scans performed at all temperatures at scattering vectors far from the Bragg reflections. The resolution function is composed of a strong Gaussian with FWHM=80 μeV (pure instrumental resolution) and a weak Lorentzian line with FWHM =2 meV centered at zero energy transfer (caused by incoherent scattering from water adsorbed at the nanoparticles and fluctuations of disordered surface spins[53]). Furthermore, an asymmetry is included for $\varepsilon < 0$ meV, caused by the BeO filter, which blocks elastically scattered (background-causing) neutrons at settings with $\varepsilon > 0.05$ meV. In the fitting procedure the obtained resolution function was convoluted with the expressions for the superparamagnetic relaxation and the collective magnetic excitations [Eqs. (5) and (6)], and a linear background with constant slope was added.

IV. EXPERIMENTAL RESULTS

A. Results from inelastic neutron scattering

Figures 2 and 3 show examples of the inelastic neutron scattering data obtained for a constant scattering vector at $Q=\tau_{003}=1.37$ Å^{-1}. In all figures the filled circles represent the data for the noninteracting nanoparticles and the open circles represent the interacting nanoparticles. The measurements were performed in the temperature range 5–300 K and in applied magnetic fields up to 10 T perpendicular to the incoming neutron beam and to the neutron scattering vector.

Figures 2(a) and 2(b) show the data for the noninteracting nanoparticles at T=10 and 150 K, respectively, including the fit to the model represented by the thin line. At the highest temperature the inelastic peaks have a large intensity indicating an increased population of the uniform magnetic excitations. The related part of the fit is shown by the bold line. Similar data for the interacting nanoparticles are shown in Figs. 2(c) and 2(d) for the temperatures T=5 and 150 K, respectively. The inelastic signal is less pronounced and appears considerably broadened as compared to the data for the noninteracting nanoparticles.

Figures 3(b) and 3(d) show the inelastic neutron scattering signal at T=100 K when a magnetic field of 6 T has been applied. Figures 3(a) and 3(c) show the corresponding zero field scans. It can be seen that application of a magnetic field increases the excitation energy in both samples. This is quali-

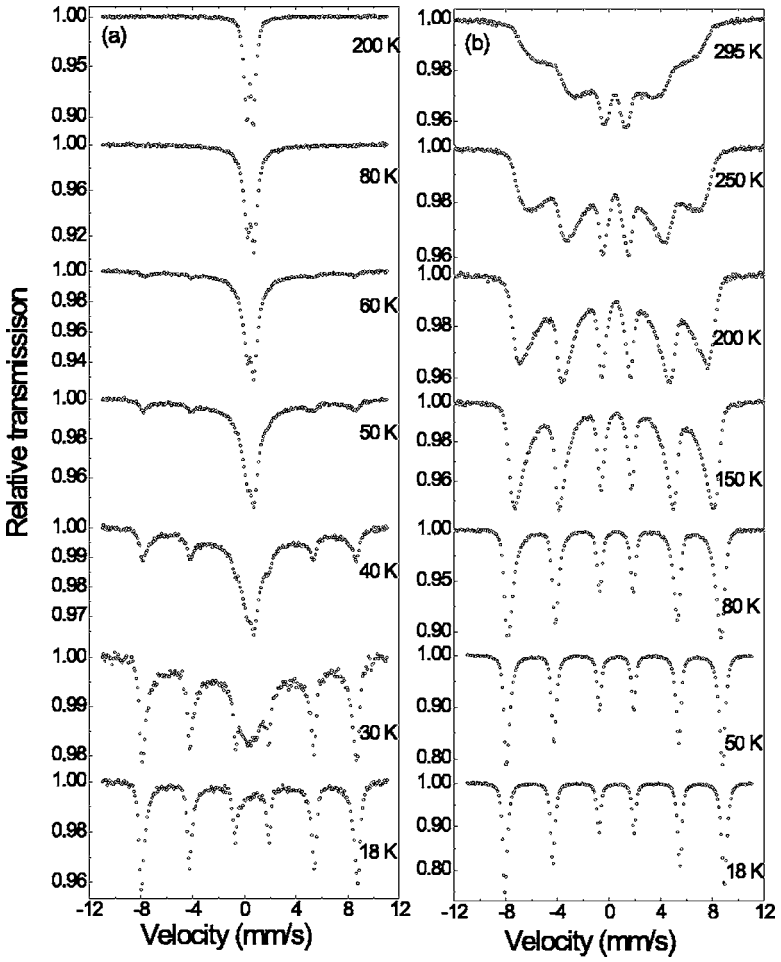

FIG. 4. Mössbauer spectra of the 8-nm α -Fe_2O_3 nanoparticles at various temperatures from 18 K to room temperature. (a) Data for the noninteracting particles and (b) data for the interacting particles.

tatively in accordance with Eq. (8). The broad inelastic components associated with the collective magnetic excitations are absent for data taken at nonmagnetic values of the scattering vector (data not shown).

B. Results from Mössbauer spectroscopy

Mössbauer spectra of the noninteracting and interacting particles, obtained at various temperatures, are shown in Fig. 4. The spectra of the coated nanoparticles [Fig. 4(a)] show a superparamagnetic behavior typical for noninteracting or weakly interacting nanoparticles.[33,35,36] At 18 K the spectrum consists of a sextet with narrow lines, indicating that at this temperature essentially all nanoparticles in the sample have relaxation times longer than the time scale of Mössbauer spectroscopy (i.e., $\geqslant 5\times 10^{-9}$ s). As the temperature is increased, a doublet appears in the spectra. This doublet is due to nanoparticles with a relaxation time shorter than the time scale of Mössbauer spectroscopy. The relative area of the doublet increases with increasing temperature, and at temperatures above 80 K the contribution from the sextet has disappeared. The spectra show a weak asymmetry of the sextet lines indicating that the coated nanoparticles may actually be weakly interacting.[33,35,36] The spectra of the interacting particles [Fig. 4(b)] show a completely different evolution with increasing temperature. Instead of the appearance of a doublet, the spectra show a substantial asymmetrical broadening of the lines of the sextet at temperatures up to room temperature. This is typical for Mössbauer spectra of interacting magnetic nanoparticles for which the energy is given by Eq. (4) and the relaxation may be described as fluctuations around a direction (mainly defined by the interaction field) rather than fluctuations between two equivalent minima at $\theta=0$ and $\theta=\pi$.[33–36]

V. DISCUSSION

We have applied the damped harmonic oscillator model to fit the inelastic neutron scattering spectra. Some of the parameters, obtained from the fits, are presented in Figs. 5, 7, and 8.

Around 200 K, the character of the relaxation changes. Well below this temperature, the dynamics can be described as a combination of uniform excitations with small amplitude (which give rise to the inelastic peaks) and superparamagnetic relaxation, i.e., reversal of the sublattice magnetization vectors (which gives rise to a broadening of the quasielastic peak). At temperatures of the order of 200 K, the thermal energy becomes comparable to the anisotropy energy, and then the two types of magnetic dynamics cannot be clearly separated because the sublattice magnetization vectors can fluctuate with similar probabilities in all directions. This isotropic relaxation regime[49] will be discussed

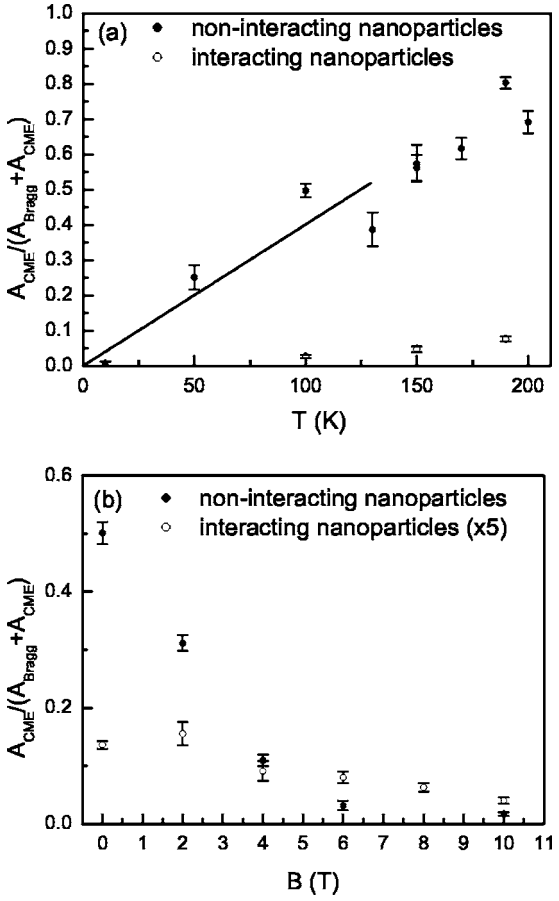

FIG. 5. The area fraction as a function of (a) temperature and (b) field at $T=100$ K. The fit to Eq. (9), which only applies at low temperatures, is shown by the solid line in (a). The data points for the interacting nanoparticles in (b) have been multiplied by 5 for clarity.

elsewhere.[48] Therefore, we will here only discuss the results obtained for $T<200$ K.

We have investigated the influence of a size distribution of the particles by weighting the inelastic neutron intensity with a log-normal size distribution (with standard deviation $\sigma=0.5$) and letting the anisotropy vary with size according to the findings of Ref. 31. For the nanoparticle sizes in this study it only introduces minor modifications, we therefore here present the analysis in which we have assumed monodisperse particles.

A. The magnetic anisotropy and interaction energies

The relative area of the inelastic peaks as compared to the total magnetic scattering, $A_{\mathrm{CME}}/(A_{\mathrm{Bragg}}+A_{\mathrm{CME}})$, as a function of temperature and applied field is shown in Figs. 5(a) and 5(b), respectively. For both samples, the relative area of the inelastic peaks increases with temperature, but the effect is strongest for the noninteracting particles. We have fitted the low-temperature data for the noninteracting particles with Eq. (9) yielding an estimate of the effective anisotropy of $K_{\mathrm{eff}}V/k_B=250(30)$ K $[K_{\mathrm{eff}}=1.3(2)\times10^4$ J/m$^3]$ for the noninteracting nanoparticles. The data for the interacting particles

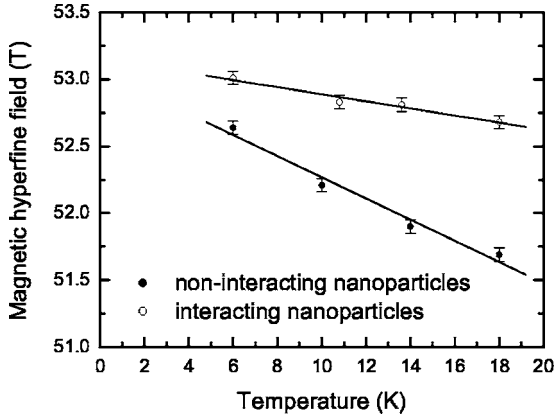

FIG. 6. The average observed hyperfine field $\langle B_{\mathrm{obs}}\rangle$ obtained from the Mössbauer data, as a function of temperature. The lines are linear fits to the data.

show a much smaller relative area of the inelastic peaks than for the noninteracting particles. Application of a magnetic field decreases the inelastic signal from the noninteracting nanoparticles, whereas only magnetic fields larger than about 3 T have a measurable effect on the interacting nanoparticles.

We have fitted the low-temperature Mössbauer spectra to estimate the average hyperfine field $\langle B_{\mathrm{obs}}\rangle$ at temperatures up to 18 K, i.e., in a range where the superparamagnetic relaxation of most particles are blocked, but the spectra are influenced by collective magnetic excitations. The temperature dependence of $\langle B_{\mathrm{obs}}\rangle$ is shown in Fig. 6. From the linear fits we find from Eq. (10) $K_{\mathrm{eff}}V/k_B=335(35)$ K $[K_{\mathrm{eff}}=1.7(2)\times10^4$ J/m$^3]$ for the noninteracting particles, which is in good agreement with the value found from the neutron data. For the interacting particles we find from Eq. (11) $(2K_{\mathrm{eff}}V+E_{\mathrm{int}})/k_B=1330(180)$ K. Assuming K_{eff}V to be the same for the two samples, we obtain $E_{\mathrm{int}}/k_B=660(200)$ K.

In α-Fe_2O_3 the different superexchange coupling constants are in the range 10–30 K,[44] For Fe^{3+} ions with spin $s=5/2$ this corresponds to an exchange energy per exchange bridge in the range 60–190 K. Therefore only a few (of the order of ten) exchange bridges between neighboring α-Fe_2O_3 nanoparticles are needed to account for the observed interaction effects. Similar values were estimated from Mössbauer data for interacting 20 nm α-Fe_2O_3 nanoparticles.[33]

B. The energy related to the uniform precession states

The measured dynamic behavior of the 8-nm hematite nanoparticles show several interesting effects, which were not observed in previous studies of larger particles.[7,39,43] First we discuss data for the noninteracting nanoparticles. The excitation energy ε_0 shows a weak linear increase with temperature [Fig. 7(a)]. Extrapolating ε_0 to $T=0$ K gives $\varepsilon_{0,T=0}=0.214(5)$ meV. The increase of ε_0 with increasing temperature is surprising since the damped harmonic oscillator model predicts a decreasing ε_0, which was also observed for larger 15-nm α-Fe_2O_3 nanoparticles.[39,43] Furthermore,

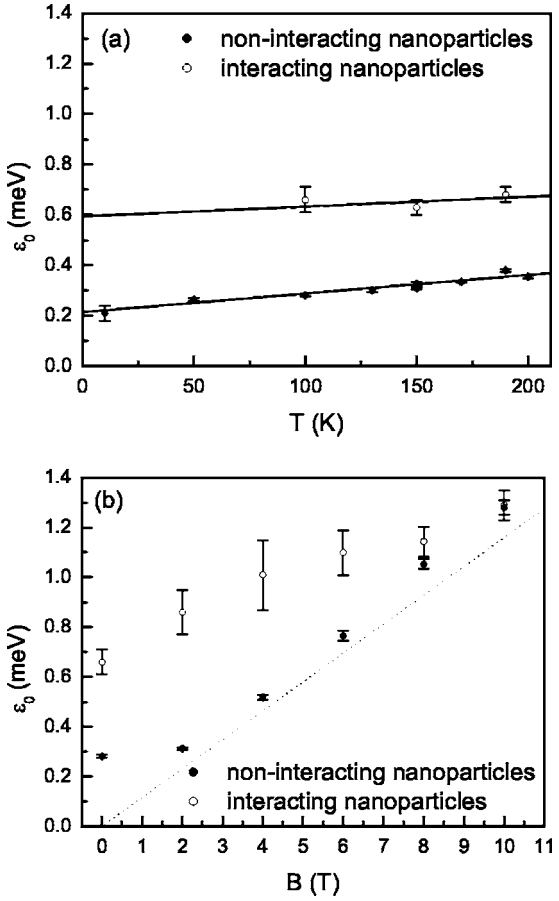

FIG. 7. Position of the inelastic peaks as a function of (a) temperature and (b) field at $T=100$ K. The solid lines in (a) show the linear extrapolation to $T=0$ K and in (b) the dotted line represents Eq. (8).

because the magnetic anisotropy constant of α-Fe_2O_3 nanoparticles increases with decreasing particle size[31] one would expect an increasing $\varepsilon_{0,T=0}$ with decreasing particle size, and this is also opposite to the present observation (for 15-nm α-Fe_2O_3 nanoparticles $\varepsilon_{0,T=0}=0.26$ meV).[39]

It is known[17,18] that antiferromagnetic nanoparticles usually have an uncompensated magnetic moment, with a relative size increasing with decreasing particle size. One can show that the equation of motion for the $q=0$ mode in a microscopic model for a particle with different number of spins in two sublattices is equivalent to that of two interacting macrospins.[54] Thus nanoparticles of antiferromagnetic materials should in principle be described as ferrimagnets with a very small difference ΔM between the sublattice magnetic moments. Even a small uncompensated moment can have a significant influence on the precession frequency of the uniform mode. Introducing the relative uncompensated moment $\zeta=\Delta M/M_s$ in one sublattice, Eq. (7) should be replaced by[55–58]

$$\varepsilon_0^{1,2}=\frac{1}{2}g\mu_B B_E[\sqrt{4\lambda^2+4\lambda(2+\zeta)+\zeta^2}\pm\zeta]. \qquad (12)$$

Here $\lambda=K_{\text{eff}}/(B_E M_s)$. We have assumed that the magnetic anisotropy is uniaxial and given by Eq. (1) and that the spin structure and the precession modes are not influenced by, for example, surface effects in the nanoparticles. In previous work on 15-nm α-Fe_2O_3 particles[7,39,43] the influence of an uncompensated moment on the precession frequency was not observed. However, in the 8-nm particles studied here, the relative uncompensated moment is expected to be larger and therefore to have a stronger influence on ε_0, and this may explain the small value of ε_0 and its anomalous temperature dependence. Inserting the measured value of $\varepsilon_{0,T=0}=0.214$ meV and using the estimated $K_{\text{eff}}=1.3\times10^4$ J/m^3 (obtained in Sec. V A) and assuming that the low-energy mode (ε_0^1) is predominant, we determine an uncompensated moment $\Delta M/M_{s,T=0}\approx1.1\%$. According to Eq. (12), the other mode with higher frequency (ε_0^2) then corresponds to $\varepsilon_{0,T=0}\approx1.7$ meV. We do not resolve the neutron intensity from this mode because it is significantly reduced in comparison to mode ε_0^1.

It should be emphasized that the use of the simple expression Eq. (1) for the magnetic anisotropy energy, which was also used in previous neutron studies of hematite nanoparticles,[39,43] is only a first order approximation. Both in bulk hematite and hematite nanoparticles, the sublattice magnetization is to a large extent confined to the (001) plane because of a large out-of-plane anisotropy with anisotropy constant K_1. The smaller in-plane anisotropy, K_{Bu} has been found to increase with decreasing particle size.[31] In neutron studies of the high-frequency and low-frequency modes in 15 nm particles the values $K_1=5\times10^4$ J/m^3 and $K_{\text{Bu}}=0.3\times10^4$ J/m^3 were estimated, but from the results above we estimate that K_{Bu} is larger in the present 8-nm particles. Unfortunately, the value of K_1 in 8-nm particles is not known, because we were unable to detect the high-frequency mode, and therefore we are not able to perform a more rigorous data analysis. However, it is likely that K_1 and K_{Bu} are of the same order of magnitude in the 8 nm particles, and therefore Eq. (1) may be a fair approximation to the magnetic anisotropy energy.

Néel[17,18] suggested some simple models for estimating the uncompensated moment. In one model, he assumed that the interior of the nanoparticle is essentially free of defects, but that the surface sites are randomly occupied such that the number of uncompensated spins is of the order of the square root of the number of surface spins. For the present particles this would give a fraction of uncompensated spins of about 0.8% in one sublattice, which is close to the value estimated from the experimental data $\approx1.1\%$.

Mössbauer spectroscopy with large magnetic fields applied to the sample can give information on the relative importance of the magnetic moments due to canting and to uncompensated spins. Such studies of 15-nm hematite particles showed that the moment due to uncompensated spins was small compared to the moment due to canting.[59] We have made similar measurements on the 8-nm particles and found that the two contributions in this case are of the same order of magnitude, i.e., the relative importance of the uncompensated spins is larger in this case.

The nanoparticles with an uncompensated moment may be considered as weak ferrimagnets. However, the dipole interaction energy, even between two particles in contact, is very weak ($\lesssim1$ K).[33] Thus, the interaction effects observed

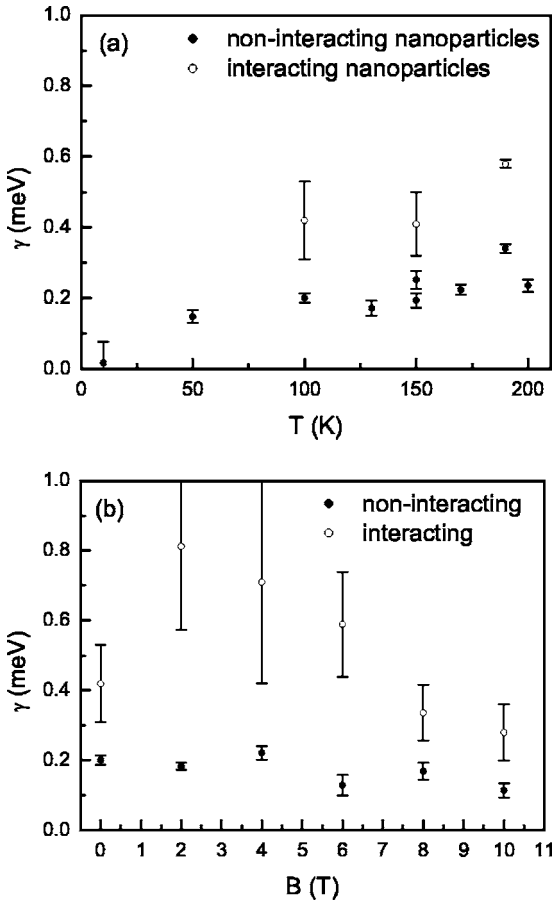

FIG. 8. Width of the inelastic peaks as a function of (a) temperature and (b) field at $T=100$ K.

in the interacting particles must be explained by exchange interactions.

When a magnetic field is applied [Fig. 5(b)] the amplitude of the inelastic peak decreases. This can be explained by the increase of the excitation energy of the precession modes, which results in a decrease of the thermal populations. ε_0 increases for the noninteracting nanoparticles at all fields up to 10 T. At large applied fields $\varepsilon_0(B)$ follows the behavior predicted by Eq. (8), which is shown by the dotted line in Fig. 7(b) (assuming[39] $g=2$).

The width γ of the inelastic peak increases with temperature [Fig. 8(a)]. Though the values are comparable, this increase with temperature is opposite to what was seen in previous experiments on 15-nm α-Fe_2O_3 nanoparticles.[39,43] Theoretically, it has been predicted that the width first decreases with temperature and then at a certain critical temperature starts to increase.[45] This is caused by the balance between the anisotropy energy barrier and the sublattice exchange interaction in α-Fe_2O_3. For the present experiments the anisotropy energy of the 8-nm α-Fe_2O_3 nanoparticles may be such that we have entered the regime where an increase in width is possible. For the interacting nanoparticles the width is a factor 2–3 larger indicating that there is a broad range of interaction energies.

Applying a magnetic field [Fig. 8(b)] reduces the width. The magnetic field narrows the range of frequencies and suppresses to some extent the amplitude of the excitations.

Now we discuss the corresponding measurements for the interacting particles. The temperature dependence of ε_0 is similar to that of the noninteracting particles. For the interacting nanoparticles, ε_0 [Fig. 7(b)] starts at a higher value for low magnetic fields $\varepsilon_0(B=0)\approx 0.65$ meV and reaches the value for the noninteracting nanoparticles at 10 T. The field dependence of ε_0 shows a significant deviation from Eq. (8) for fields up to 8 T. Thus the interaction energy is predominant and we estimate that the effective interaction field is of the order of 5 T. On the other hand, E_{int} can be considered as a product of this interaction field and an effective moment. For $E_{\text{int}}\approx 660$ K one can estimate an effective moment of 130 Bohr magnetons, which would correspond to about 50 iron atoms. The behavior of γ for the interacting nanoparticles starts to approach that of the weakly interacting nanoparticles at an applied field of 5 T, in accordance with the previous findings.

VI. CONCLUSION

Using inelastic neutron scattering we have studied the collective magnetic excitations in noninteracting and interacting 8-nm α-Fe_2O_3 nanoparticles. The data are well described by the damped harmonic oscillator model. The determined characteristic energy ε_0 suggests that the magnetic properties of the 8-nm α-Fe_2O_3 nanoparticles are strongly affected by an uncompensated moment in one sublattice of $\Delta M/M_{s,T=0}\approx 1.1\%$, which is present as a finite size effect in the antiferromagnetic nanoparticles. The collective magnetic excitations are strongly influenced by the interparticle exchange interactions, and from Mössbauer spectroscopy data we have estimated the interaction energy E_{int}/k_B to be approximately 660 K. This energy corresponds to in average a few exchange bridges between the α-Fe_2O_3 nanoparticles. This is supported by the neutron measurements. We conclude that inelastic neutron scattering besides probing spin dynamics in magnetic nanoparticles also can add important information on uncompensated moments and interparticle interactions.

ACKNOWLEDGMENTS

We thank F. Bødker for preparing the α-Fe_2O_3 nanoparticles. We have had many clarifying discussions with B. Lebech for which we are grateful. The work was supported by the Danish Technical Research Council through the framework program on nanomagnetism, and the Danish Natural Science Research Council through the Danish Neutron Scattering Centre, DANSCATT. The electron microscopy was carried out at the Danish TEM Centre, supported by the Danish Natural Science and Technical Research Councils. This work is based on experiments performed at the SINQ neutron source at the Paul Scherrer Institute, Villigen, Switzerland.

*Electronic address: luise.theil.kuhn@risoe.dk
†Author to whom correspondence should be addressed.
‡Electronic address: christian.bahl@risoe.dk
§Present address: Materials Science Div., Argonne National Laboratory, Argonne, IL 60439, USA.

[1] *Fifth International Conference on Fine Particle Magnetism*, edited by Q. Pankhurst, Journal of Physics: Conference Series 17, (2005).
[2] M. P. Morales, S. A. Walton, L. S. Prichard, C. J. Serna, D. P. E. Dickson, and K. O'Grady, J. Magn. Magn. Mater. **190**, 357 (1998).
[3] L. Néel, Ann. Geophys. (C.N.R.S.) **5**, 99 (1949).
[4] S. Mørup and H. Topsøe, Appl. Phys. **11**, 63 (1976).
[5] S. Mørup, J. Magn. Magn. Mater. **37**, 39 (1983).
[6] P. V. Hendriksen, S. Linderoth, and P.-A. Lindgård, Phys. Rev. B **48**, 7259 (1993).
[7] S. N. Klausen, K. Lefmann, P.-A. Lindgård, L. Theil Kuhn, C. R. H. Bahl, C. Frandsen, S. Mørup, B. Roessli, N. Cavadini, and C. Niedermayer, Phys. Rev. B **70**, 214411 (2004).
[8] S. Mørup and B. R. Hansen, Phys. Rev. B **72**, 024418 (2005).
[9] J. L. Dormann, L. Bessais, and D. Fiorani, J. Phys. C **21**, 2015 (1988).
[10] S. Mørup and E. Tronc, Phys. Rev. Lett. **72**, 3278 (1994).
[11] P. E. Jönsson and J. L. García-Palacios, Europhys. Lett. **55**, 418 (2001).
[12] Ò. Iglesias and A. Labarta, Phys. Rev. B **70**, 144401 (2004).
[13] J. Zhang, C. Boyd, and W. Luo, Phys. Rev. Lett. **77**, 390 (1996).
[14] C. Djurberg, P. Svedlindh, P. Nordblad, M. F. Hansen, F. Bødker, and S. Mørup, Phys. Rev. Lett. **79**, 5154 (1997).
[15] H. Mamiya, I. Nakatani, and T. Furubayashi, Phys. Rev. Lett. **80**, 177 (1998).
[16] D. Fiorani, J. L. Dormann, R. Cherkaoui, E. Tronc, F. Lucari, F. D'Orazio, L. Spinu, M. Nogues, A. Garcia, and A. M. Testa, J. Magn. Magn. Mater. **196–197**, 143 (1999).
[17] L. Néel, C. R. Hebd. Seances Acad. Sci. **252**, 4075 (1961).
[18] L. Néel, in *Low Temperature Physics*, edited by C. Dewitt, B. Dreyfus, and P. D. de Gennes (Gordon & Breach, New York, 1962), p. 420.
[19] S. Mørup and C. Frandsen, Phys. Rev. Lett. **92**, 217201 (2004).
[20] M. S. Seehra, V. S. Babu, A. Manivannan, and J. W. Lynn, Phys. Rev. B **61**, 3513 (2000).
[21] J. G. E. Harris, J. E. Grimaldi, D. D. Awschalom, A. Chiolero, and D. Loss, Phys. Rev. B **60**, 3453 (1999).
[22] S. H. Kilcoyne and R. Cywinski, J. Magn. Magn. Mater. **140–144**, 1466 (1995).
[23] S. A. Makhlouf, F. T. Parker, and A. E. Berkowitz, Phys. Rev. B **55**, R14717 (1997).
[24] N. J. O. Silva, V. S. Amaral, and L. D. Carlos, Phys. Rev. B **71**, 184408 (2005).
[25] B. Barbara and E. M. Chudnovsky, Phys. Lett. A **145**, 205 (1990).
[26] J. Tejada and X. X. Zhang, J. Phys.: Condens. Matter **6**, 263 (1994).
[27] M. Duran, E. del Barco, J. M. Hernandez, and J. Tejada Phys. Rev. B **65**, 172401 (2002).
[28] E. del Barco, M. Duran, J. M. Hernandez, J. Tejada, R. D. Zysler, M. Vasquez Mansilla, and D. Fiorani, Phys. Rev. B **65**, 052404 (2002).
[29] R. H. Kodama, S. A. Makhlouf, and A. E. Berkowitz, Phys. Rev. Lett. **79**, 1393 (1997).
[30] W. Kündig, K. J. Ando, G. Constabaris, and R. H. Lindquist, Phys. Rev. **142**, 327 (1966).
[31] F. Bødker and S. Mørup, Europhys. Lett. **52**, 217 (2000).
[32] R. D. Zysler, D. Fiorani, A. M. Testa, L. Suber, E. Agostinelli, and M. Godinho, Phys. Rev. B **68**, 212408 (2003).
[33] M. F. Hansen, C. B. Koch, and S. Mørup, Phys. Rev. B **62**, 1124 (2000).
[34] S. Mørup, M. B. Madsen, J. Franck, J. Villadsen, and C. J. W. Koch, J. Magn. Magn. Mater. **40**, 163 (1983).
[35] S. Mørup, C. Frandsen, F. Bødker, S. N. Klausen, K. Lefmann, P.-A. Lindgård, and M. F. Hansen, Hyperfine Interact. **144/145**, 347 (2002)
[36] C. Frandsen and S. Mørup, J. Magn. Magn. Mater. **266**, 36 (2003).
[37] C. Frandsen and S. Mørup, Phys. Rev. Lett. **94**, 027202 (2005).
[38] F. Gazeau, E. Dubois, M. Hennion, R. Perzynski, and Y. Raikher, Europhys. Lett. **40**, 575 (1997).
[39] M. F. Hansen, F. Bødker, S. Mørup, K. Lefmann, K. N. Clausen, and P.-A. Lindgård, Phys. Rev. Lett. **79**, 4910 (1997).
[40] K. Lefmann, F. Bødker, M. F. Hansen, H. Vázquez, N. B. Christensen, P.-A. Lindgård, K. N. Clausen, and S. Mørup, Eur. Phys. J. D **9**, 491 (1999).
[41] M. F. Hansen, F. Bødker, S. Mørup, K. Lefmann, K. N. Clausen, and P.-A. Lindgård, J. Magn. Magn. Mater. **221**, 10 (2000).
[42] K. Lefmann, F. Bødker, S. N. Klausen, M. F. Hansen, K. N. Clausen, P.-A. Lindgård, and S. Mørup, Europhys. Lett. **54**, 526 (2001).
[43] S. N. Klausen, K. Lefmann, P.-A. Lindgård, K. N. Clausen, M. F. Hansen, F. Bødker, S. Mørup, and M. Telling, J. Magn. Magn. Mater. **266**, 68 (2003).
[44] A. H. Morrish, *Canted Antiferromagnetism: Hematite* (World Scientific, Singapore, 1994).
[45] J. D. Lee, Phys. Rev. B **70**, 174450 (2004).
[46] T. Sugimoto, Y. Wang, H. Itoh, and A. Muramatsu, Colloids Surf., A **134**, 265 (1998).
[47] C. Frandsen, C. R. H. Bahl, B. Lebech, K. Lefmann, L. Theil Kuhn, L. Keller, N. H. Andersen, M. v. Zimmermann, E. Johnson, S. N. Klausen, and S. Mørup, Phys. Rev. B **72**, 214406 (2005).
[48] L. Theil Kuhn, K. Lefmann, C. R. H. Bahl, S. N. Klausen, A. Wischnewski, C. Frandsen, and S. Mørup (unpublished).
[49] A. Würger, Europhys. Lett. **44**, 103 (1998).
[50] E. Tronc and J. P. Jolivet, Hyperfine Interact. **28**, 525 (1986).
[51] S. N. Klausen, K. Lefmann, D. F. McMorrow, F. Altorfer, S. Janssen, and M. Luthy, Appl. Phys. A: Mater. Sci. Process. **74**, S1508 (2002); see also the home page http://sinq.web.psi.ch/sinq/instr/rita2
[52] K. Lefmann, D. F. McMorrow, H. M. Rønnow, K. Nielsen, K. N. Clausen, B. Lake, and G. Aeppli, Physica B **283**, 343 (2000).
[53] L. Theil Kuhn, K. Lefmann, S. N. Klausen, H. M. Rønnow, A. Murani, and R. Stewart, Physica B **350**, e217 (2004).
[54] C. R. H. Bahl, K. Lefmann, T. B. S. Jensen, P.-A. Lindgård, D. E. Madsen, and S. Mørup (unpublished)
[55] A. H. Morrish, *The Physical Principles of Magnetism* (Wiley, New York, 1965).
[56] C. Kittel, Phys. Rev. **82**, 565 (1951).
[57] F. Keffer and C. Kittel, Phys. Rev. **85**, 329 (1952).
[58] R. K. Wangsness, Phys. Rev. **86**, 146 (1952); **91**, 1085 (1953).
[59] F. Bødker, M. F. Hansen, C. B. Koch, K. Lefmann, and S. Mørup, Phys. Rev. B **61**, 6826 (2000).